J Biomol NMR (2013) 55:71–78
DOI 10.1007/s10858-012-9689-3

ARTICLE

The protein amide $^{1}H^{N}$ chemical shift temperature coefficient reflects thermal expansion of the N–H···O=C hydrogen bond

Jingbo Hong · Qingqing Jing · Lishan Yao

Received: 15 August 2012 / Accepted: 22 November 2012 / Published online: 1 December 2012

Abstract The protein amide $^{1}H^{N}$ chemical shift temperature coefficient can be determined with high accuracy by recording spectra at different temperatures, but the physical mechanism responsible for this temperature dependence is not well understood. In this work, we find that this coefficient strongly correlates with the temperature coefficient of the through-hydrogen-bond coupling, $^{3h}J_{NC'}$, based on NMR measurements of protein GB3. Parallel tempering molecular dynamics simulation suggests that the hydrogen bond distance variation at different temperatures/replicas is largely responsible for the $^{1}H^{N}$ chemical shift temperature dependence, from which an empirical equation is proposed to predict the hydrogen bond thermal expansion coefficient, revealing responses of individual hydrogen bonds to temperature changes. Different expansion patterns have been observed for various networks formed by β strands.

Keywords Amide proton · GB3 · Chemical shift temperature coefficient · Molecular dynamics simulation · Hydrogen bond

Introduction

NMR chemical shifts enable one to distinguish signals from nuclei in different environments, thereby providing important structural information. Significant progress has been made to understand the chemical shift/structure relationship for proteins, so that one can now predict chemical shifts with reasonable accuracy from a known structure (Kohlhoff et al. 2009; Neal et al. 2003; Shen and Bax 2007, 2010; Vila et al. 2008; Xu and Case 2001) or calculate a protein structure based on chemical shifts in combination with other NMR or computational restraints (Cavalli et al. 2007; Shen et al. 2008, 2009; Vila et al. 2008). Chemical shifts are sensitive to structural as well as environmental effects. It is well known that a minor temperature perturbation can cause changes in chemical shifts. Chemical shifts can often be measured at very high precision which allows the accurate determination of small temperature coefficients for various nuclei, e.g. protein backbone amide $^{1}H^{N}$, ^{15}N, $^{13}C^{\alpha}$ and etc. Unlike chemical shifts themselves, these coefficients are poorly understood. The purpose of this work is to obtain an improved understanding of the $^{1}H^{N}$ chemical shift temperature coefficient, and its relationship to protein structure.

Before identifying what determines the $^{1}H^{N}$ chemical shift temperature coefficient, one has to take a step back to understand what factors impact the amide $^{1}H^{N}$ chemical shift itself. The protein amide $^{1}H^{N}$ chemical shift depends upon numerous factors, e.g. hydrogen bonds, ring-currents, peptide magnetic anisotropies and electrostatic interactions (Sitkoff and Case 1997). The hydrogen bond effect on the amide $^{1}H^{N}$ chemical shift has been well studied computationally (Barfield 2002; Parker et al. 2006) and experimentally (Cordier and Grzesiek 1999). Qualitatively, the hydrogen bond polarizes the electron density along the N–H direction, perturbs the induced magnetic field along directions perpendicular to the N–H axis, and thus decreases their shielding. As a result, the shielding components perpendicular to the N–H axis are reduced more by

Electronic supplementary material The online version of this article (doi:10.1007/s10858-012-9689-3) contains supplementary material, which is available to authorized users.

J. Hong · Q. Jing · L. Yao (✉)
Laboratory of Biofuels, Qingdao Institute of Bioenergy and Bioprocess Technology, Chinese Academy of Sciences, Qingdao 266061, China
e-mail: yaols@qibebt.ac.cn

the hydrogen bond interaction than that along the N–H axis. The overall effect is that a stronger hydrogen bonded amide $^{1}H^{N}$ has a smaller shielding thus a more down field chemical shift. It has been suggested that a direct hydrogen bond has a dominant effect on the $^{1}H^{N}$ chemical shift (Parker et al. 2006).

There are a few published $^{1}H^{N}$ temperature coefficient studies, where the temperature coefficient has been generally linked to the $^{1}H^{N}$ formed hydrogen bond (Baxter and Williamson 1997; Cierpicki and Otlewski 2001; Cierpicki et al. 2002). Amides involved in strong intramolecular hydrogen bonds tend to have less negative temperature coefficients than those weakly h-bonded to water. However in a more recent study, a poor correlation has been observed for the $^{1}H^{N}$ temperature coefficient and the hydrogen bond distance, implying that the temperature coefficient is a poor indicator of hydrogen bond strength (Tomlinson and Williamson 2012). A strong correlation has been observed for peptides between the $^{1}H^{N}$ temperature coefficient and the $^{1}H^{N}$ secondary shift (defined as the deviation from the random coil chemical shift value; Andersen et al. 1997) while the same correlation is much weaker for protein GB1 (Tomlinson and Williamson 2012). The correlation in peptides is attributed to the temperature dependent equilibrium shift between the folded and unfolded states. For a protein with the measurement temperature well below its melting temperature, the vast majority part remains folded and the equilibrium shift is very small, though certain residues may display temperature dependent conformational distribution. It has also been proposed that the $^{1}H^{N}$ temperature coefficient is due to thermal expansion of the protein. Briefly, it is suggested that the intramolecular hydrogen bonds extend with increasing temperature and the lengthening of the hydrogen bonds weakens the $^{1}H^{N}$ electron polarization, thus causing up-field movements of chemical shifts as observed experimentally for many protein $^{1}H^{N}$ nuclei. Considering the importance of hydrogen bonds upon the $^{1}H^{N}$ chemical shift, this is likely true, as implied by early studies (Baxter and Williamson 1997; Cordier and Grzesiek 2002; Tomlinson and Williamson 2012), but has not been thoroughly examined. The through hydrogen bond J-coupling, $^{3h}J_{NC'}$, provides a direct measure of protein backbone N–H···O=C hydrogen bond (Cordier and Grzesiek 1999; Cornilescu et al. 1999a, b), and has been used to study the hydrogen bond expansion of protein ubiquitin (Cordier and Grzesiek 2002). It is a good tool for the purpose.

This paper is organized as follows: First, we demonstrate that the temperature coefficients of amide $^{1}H^{N}$ chemical shifts and $^{3h}J_{NC'}$ are strongly correlated. Second, we identify the hydrogen bond parameter that contributes to the $^{1}H^{N}$ chemical shift temperature coefficient based on a parallel tempering molecular dynamics simulation. Third, we propose an empirical equation to estimate the hydrogen bond expansion coefficient from the $^{1}H^{N}$ chemical shift temperature coefficient. Finally, we summarize our results and discuss the structural effect of the h-bond expansion.

Methods and materials

Sample express and purification

56-residue third IgG-binding domain of protein G, GB3, was made by expression in Escherichia Coli BL21 (DE3*) cells, transformed with a pET-11 vector containing the GB3 gene. The detailed procedure of preparation and purification was described previously (Yao et al. 2009). A ^{15}N, ^{13}C labeled NMR sample was made, containing 2 mM GB3, 50 mM sodium phosphate, 0.1 % w/v 4, 4-dimethyl-4-silapentane-1-sulfonic acid (DSS), pH 6.5 in 500 µl volume.

NMR spectroscopy

All NMR experiments were carried out on a Bruker Avance 600 MHz spectrometer, equipped with a z-axis gradient, triple resonance, cryogenic probe. 2D ^{15}N–^{1}H HSQC spectra were recorded at 288, 293, 298 and 303 K to obtain $^{1}H^{N}$ chemical shifts referenced to DSS which was set at 0 ppm at different temperatures. The acquisition times were 70.4(^{15}N) and 166 ms (^{1}H) with the data matrices consisting of 128* × 2048* data points, where N* indicates N complex points. For the through hydrogen bond $^{3h}J_{NC'}$, the pulse sequence is based on the experiment by Cornilescu et al. (1999a, b), with a minor difference that the ^{1}H decoupling during $^{3h}J_{NC'}$ evolution was turned off. The acquisition times were 48(^{13}C) and 64.9 ms (^{1}H) with the data matrices consisting of 60* × 800* data points. The reference spectra were recorded with 8 scans; the spectrum with the magnetization build-up from $^{3h}J_{NC'}$ was recorded with 256 scans. The $^{3h}J_{NC'}$ measurements were performed at 288, 293, 298, 303, 308, 313 and 318 K and at each temperature duplicate measurement was performed to estimate $^{3h}J_{NC'}$ error.

Molecular dynamics simulation

Molecular dynamics (MD) simulation was carried out using Gromacs 4.5 (Hess et al. 2008; Van der Spoel et al. 2005), the amber ff99SB force field (Hornak et al. 2006) and TIP3P water. The starting coordinates were from the GB3 structure (pdb 2OED). All residues were assumed to be in their standard ionization states at pH 7.0. The protein was solvated by adding 10.0 Å TIP3P water in a rhombic

dodecahedron box and counter ions were used to neutralize the system. The Particle-Mesh-Ewald Method (Darden et al. 1993; Essmann et al. 1995) was used to evaluate the contributions of the long-range electrostatic interactions. A nonbonded pair list cutoff of 10.0 Å was used and the nonbonded pair list was updated every 5 steps. All bonds to hydrogen atoms in the protein were constrained by using the LINC (Hess et al. 1997) algorithm whereas bonds and angles of water molecules were constrained by the SETTLE (Miyamoto and Kollman 1992) algorithm, allowing a time step of 0.002 ps. A 110 ns sixteen-replicas parallel tempering (Hansmann 1997; Sugita and Okamoto 1999) MD simulation was performed for protein GB3. The temperatures of the sixteen replicas were set optimally to achieve ~20 % exchange probability using Patriksson et al's method (Patriksson and van der Spoel 2008) (with the online server http://folding.bmc.uu.se/remd/), at 278.00, 281.30, 284.63, 288.00, 291.40, 294.83, 298.30, 301.80, 305.33, 308.91, 312.51, 316.16, 319.83, 323.55, 327.30 and 331.09 K respectively. The temperatures were controlled by a modified Berendson thermostat (Berendsen 1991). The snapshots were saved every 50 ps, with the first 10 ns simulation treated as the equilibration thus not included in the data analysis.

Results and discussion

Temperature coefficient of the $^{1}H^{N}$ chemical shift

The $^{1}H^{N}$ chemical shifts were measured at 288, 293, 298 and 303 K and referenced to DSS (0 ppm). A linear least square fit was performed for each $^{1}H^{N}$, with the slope corresponding to the chemical shift temperature coefficient. A very good linearity was observed for all amide $^{1}H^{N}$s, with representative correlations shown in Fig. 1a. It was observed for protein ubiquitin that the amide $^{1}H^{N}$ involved in intramolecular hydrogen bonding tends to have a less negative proton chemical shift temperature coefficient (Cierpicki et al. 2002). For protein GB3, the average $^{1}H^{N}$ temperature coefficient is $-2.72 \pm 1.94 \times 10^{-3}$ ppm/K for h-bonded amides and $-4.53 \pm 2.26 \times 10^{-3}$ ppm/K for non-hbonded ones (Strictly speaking, the non-hbonded amides may form hydrogen bonds with water), in accordance with ubiquitin. However, for a specific amide, it is very difficult to distinguish whether it is h-bonded or not based on its $^{1}H^{N}$ temperature coefficient alone (Fig. 2). An empirical rule (Cierpicki et al. 2002) was proposed that a $^{1}H^{N}$ is hydrogen bonded when its temperature coefficient is weaker than -4.6×10^{-3} ppm/K, seemingly not applicable to GB3 which overall has less negative temperature coefficients.

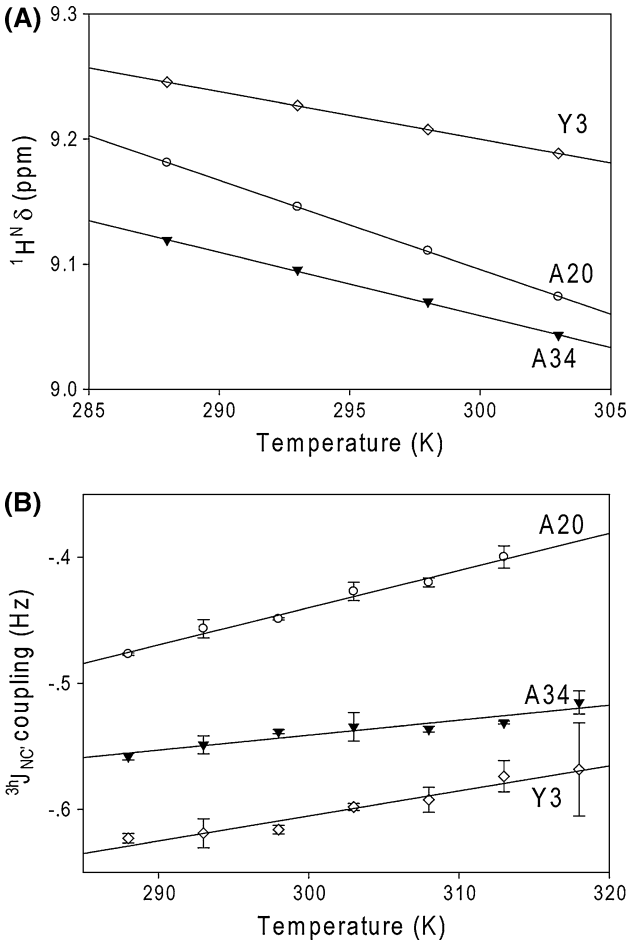

Fig. 1 **a** Correlation between the amide ^{1}H chemical shift and temperature for residues Y3, A20 and A34 of GB3. The corresponding three best fitted lines are $\delta = -5.07 \times 10^{-3}$ppm T/K + 10.58 ppm, δ (ppm) $= -7.13 \times 10^{-3}$ppm T/K + 11.24 ppm and $\delta = -3.80 \times 10^{-3}$ ppm T/K + 10.34 ppm respectively. **b** Correlation between the through hydrogen bond $^{3h}J_{NC'}$ and temperature for the same three residues, with the best fitted lines $J = 1.99 \times 10^{-3}$HzT/K − 1.20 Hz (Y3), $J = 2.95 \times 10^{-3}$HzT/K − 1.33Hz (A20) and $J = 1.19 \times 10^{-3}$ HzT/K − 0.90 Hz (A34) respectively

Temperature coefficient of $^{3h}J_{NC'}$

Values of $^{3h}J_{NC'}$ were measured at 288, 293, 298, 303, 308, 313 and 318 K. A small increase was observed for the overall $^{3h}J_{NC'}$ values, consistent with an earlier study of the protein ubiquitin (Cordier and Grzesiek 2002). The temperature coefficient of $^{3h}J_{NC'}$ for individual amide was determined by linear fit of $^{3h}J_{NC'}$ against temperature. Compared to the $^{1}H^{N}$ chemical shift, the accurate measurement of $^{3h}J_{NC'}$ is more challenging. As a result, the fitting of $^{3h}J_{NC'}$ is generally worse (Fig. 1b). Nevertheless, twenty-six $^{3h}J_{NC'}$ temperature coefficients were obtained and correlated to the corresponding $^{1}H^{N}$ temperature coefficients (Fig. 3a). A good correlation is observed with the Pearson correlation coefficient R_p 0.91. The best-fitted

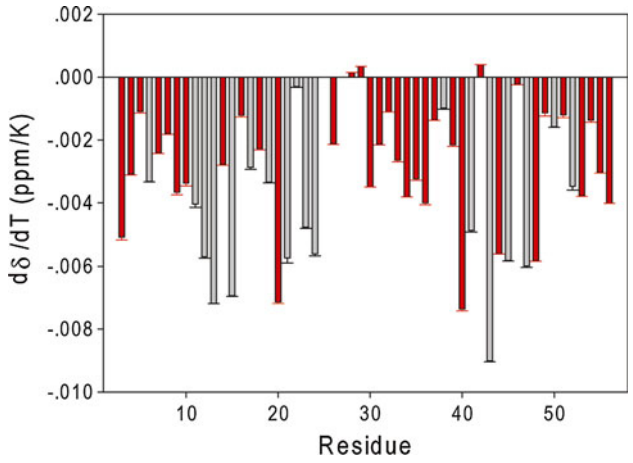

Fig. 2 Residue specific amide $^{1}H^{N}$ chemical shift temperature coefficient derived from the $^{1}H^{N}$ chemical shift measured at 288, 293, 298 and 303 K. Amide $^{1}H^{N}$s involved in intramolecular hydrogen bonds are colored in *red*, while others are in *grey*

line is dJ/dT (Hz/K) = −0.37 dδ/dT (ppm/K) + 1.28 × 10^{-4} (Hz/K). The intercept is close to zero so that dJ/dT is generally proportional to dδ/dT, suggesting the two temperature coefficients are strongly correlated and thus likely have the same origin. A similar correlation was obtained for the protein ubiquitin (Figure S1) based on the J and δ values from the literature (Cordier and Grzesiek 2002) at different temperatures. A linear correlation was observed early between J and δ with a slope of −0.33 (Cordier and Grzesiek 1999) and −0.26 ppm/K (Grzesiek et al. 2004). The number resulted from this work is slightly different. We attribute the difference mainly to the sparse data available for the fitting and the measurement inaccuracy of $^{3h}J_{NC'}$.

Origin of the two temperature coefficients

It is well known that $^{3h}J_{NC'}$ reflects the through-hydrogen-bond strength (Cornilescu et al. 1999a, b). An empirical relationship has been established (Barfield 2002; Sass et al. 2007):

$$J = 366\ \text{Hz}\ \exp(-3.2r/\text{Å})[\cos^2\theta - (0.47\cos^2\rho + 0.70\cos\rho + 0.11)\sin^2\theta \quad (1)$$

where (r, θ, ρ) are the hydrogen bond geometric parameters (Fig. 4). The hydrogen bond effect on the $^{1}H^{N}$ chemical shift has also been investigated and a similar formula has been proposed (Barfield 2002):

$$\delta = 33.78\exp(-2.0r/\text{Å})\left[4.81\cos^2\theta + (3.01\cos^2\rho - 0.84\cos\rho + 1.75)\sin^2\theta\right]\text{ppm} + 4.06\,\text{ppm} \quad (2)$$

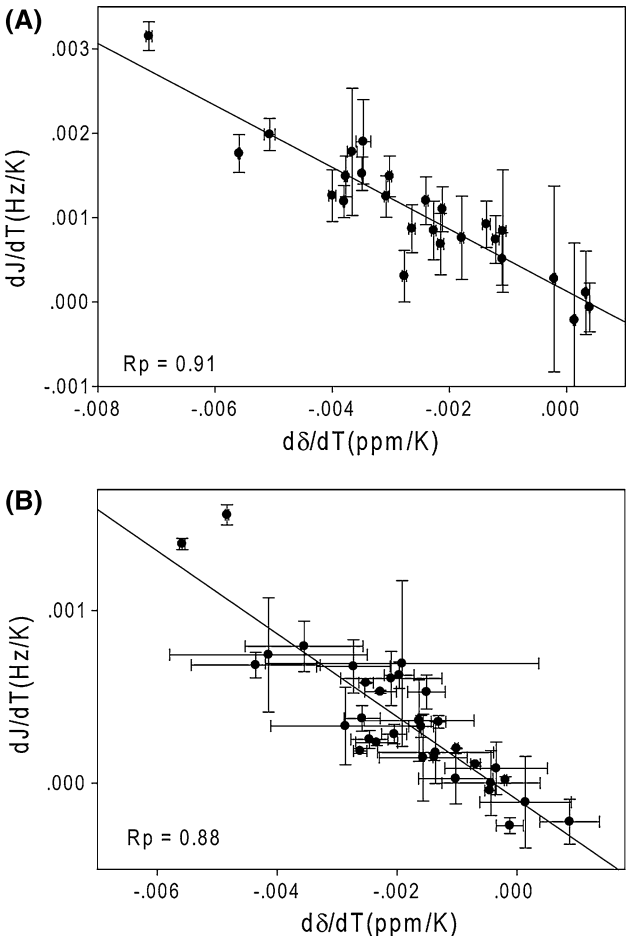

Fig. 3 Correlation between dJ/dT and dδ/dT from the experimental measurements (**a**) and the molecular dynamics simulation (**b**). dJ/dT is the through hydrogen bond $^{3h}J_{NC'}$ temperature coefficient while dδ/dT is the corresponding $^{1}H^{N}$ chemical shift temperature coefficient. The best fitted line is dJ/dT (Hz/K) = −0.37 dδ/dT (ppm/K) +1.28 × 10^{-4}Hz/K in **a**, and dJ/dT (Hz/K) = −0.24 dδ/dT (ppm/K) − 0.95 × 10^{-4}Hz/K in **b** respectively

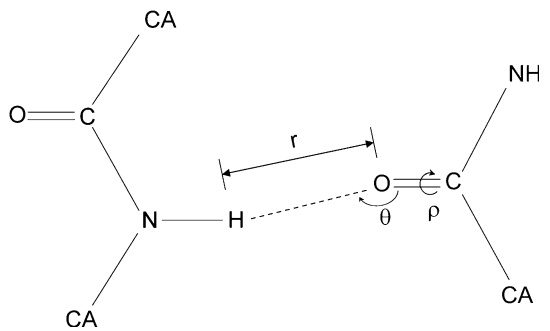

Fig. 4 Diagram of backbone amide N–H···O=C hydrogen bond, depicting geometric parameter used in Eq. 1. r denotes the distance between H and O atoms, θ is the angle ∠H–O–C, ρ is the dihedral angle H–O–C–NH

Equations 1, 2 and Fig. 3a together suggest that the $^1H^N$ chemical shift temperature coefficient arises from the perturbation of the hydrogen bond due to the temperature change.

Parallel tempering MD simulation provides detailed information about atomic motions and distributions at different temperatures, and thus is a valuable tool to study temperature dependent protein properties. A 16 replica multi temperature (spanning 278–331 K) MD simulation was performed for 110 ns. Snapshots taken during the later 100 ns were used in the data analysis. Values of $^{3h}J_{NC'}$ and $^1H^N$ chemical shifts were calculated using Eqs. 1 and 2 for the MD snapshots at different temperatures. The corresponding temperature coefficients were determined by linear least square fitting, with the errors estimated based on the difference between the first and second 50 ns trajectories. Similar to the experimental findings, a good correlation of the two types of coefficients was obtained, with R_p 0.88. The best-fit line is dJ/dT (Hz/K) $= -0.24$ $d\delta/dT$ (ppm/K) -0.95×10^{-4} (Hz/K). The intercept is close to zero in agreement with the experimental data, and the slope of -0.24 is somewhat smaller negative than the corresponding experimental value of -0.37. The correlation derived from the MD simulation is similar to the experimental one, and confirms that hydrogen bond change is responsible for the $^1H^N$ temperature coefficient. A comparison of the computational and experimental chemical shift temperature coefficients reveals a poor correlation (data not shown). This result is likely due to inaccuracy of the force field. In addition the $^1H^N$ chemical shift is extremely sensitive to local environment, so that a slight conformational space misrepresentation in the simulation can cause a large error in the calculated chemical shift and its temperature coefficient.

Equation 2 suggests that the $^1H^N$ chemical shift is determined by three geometric parameters, namely r, θ and ρ (Fig. 4) which depend upon temperature. But which one contributes the most to the $^1H^N$ chemical shift temperature coefficient? To properly address this question, one needs to know how each geometric parameter varies with temperature and how this variation transforms to $d\delta/dT$. Starting from Eq. 2, chain rule is applied to derive $d\delta/dT$:

$$\frac{d\delta}{dT} = \frac{d\delta}{dr}\cdot\frac{dr}{dT} + \frac{d\delta}{d\theta}\cdot\frac{d\theta}{dT} + \frac{d\delta}{d\rho}\cdot\frac{d\rho}{dT} \quad (3)$$

It is straightforward to derive $d\delta/dr$, $d\delta/d\theta$ and $d\delta/d\rho$ from Eq. 2. Once the formulas are established, the corresponding values can be extracted from MD simulation. In principle, $d\delta/dr$, $d\delta/d\theta$ and $d\delta/d\rho$ are functions of temperature as well, thus can be different at different temperatures. But the differences are rather small due to the fact that δ values for individual amide $^1H^N$ at different temperatures are similar, so that the values of $d\delta/dr$, $d\delta/d\theta$ and $d\delta/d\rho$ at one temperature (e.g. 298.3 K used here) can be used in Eq. 3 to transfer geometric temperature coefficients to $d\delta/dT$. The terms dr/dT, $d\theta/dT$ and $d\rho/dT$ were estimated by linear fits of the structure parameters from the MD snapshots to temperature. The contribution from each term in Eq. 3 was evaluated, with the result that $\frac{d\delta}{dr}\cdot\frac{dr}{dT}$ is the dominant term. The correlation between $d\delta/dT$ and $\frac{d\delta}{dr}\cdot\frac{dr}{dT}$ is shown in Fig. 5a, with the R_p 0.90 and the best fitted line:

$$\frac{d\delta}{dT} = a\frac{d\delta}{dr}\cdot\frac{dr}{dT} + b \quad (4)$$

The coefficient $a = 0.86$, suggests that the contributions from $d\theta/dT$ and $d\rho/dT$ are small and negative. The coefficient $b = -0.91 \times 10^{-4}$ (ppm/K), is negligibly small. Equation 4 demonstrates that the $^1H^N$ chemical shift temperature coefficient mainly arises from the hydrogen bond distance

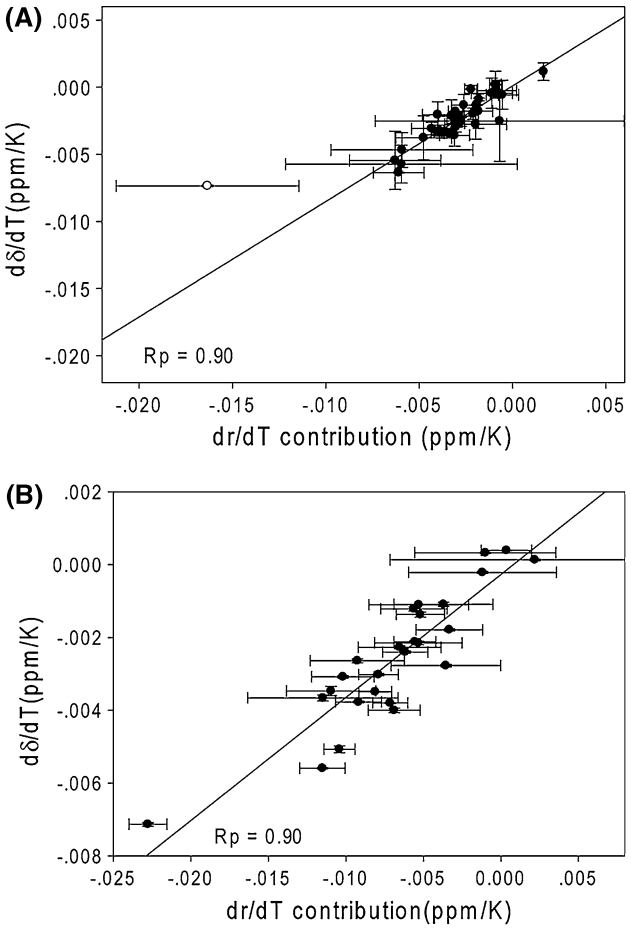

Fig. 5 Correlation between the $^1H^N$ chemical shift temperature coefficient $d\delta/dT$ and its contribution derived from the hydrogen bond distance expansion $\frac{d\delta}{dr}\cdot\frac{dr}{dT}$ for MD simulation (**a**) and experimental data (**b**). The best fitted *lines* are $d\delta/dT$ (ppm/K) $= 0.86\ \frac{d\delta}{dr}\cdot\frac{dr}{dT}$ (ppm/K) $- 0.91\times10^{-4}$ ppm/K for A (excluding one outlier), and $d\delta/dT$ (ppm/K) $= 0.34\ \frac{d\delta}{dr}\cdot\frac{dr}{dT}$ (ppm/K) $- 2.7\times10^{-4}$ ppm/K for B

change. The temperature coefficient of $^{3h}J_{NC'}$ is also dominated by the distance change (Figure S2).

Estimation of the hydrogen bond distance temperature coefficient

Using Eq. 4, one can estimate the coefficient dr/dT from dδ/dT if the quantity dδ/dr is known. From Eq. 2, one gets:

$$\mathrm{d}\delta/\mathrm{dr} = -2(\delta - 4.06\mathrm{ppm})/\text{Å} \tag{5}$$

Combining Eqs. 4 and 5 yields:

$$\frac{\mathrm{d}\delta}{\mathrm{dT}} = -0.862(\delta - 4.06\mathrm{ppm}) \cdot \frac{\mathrm{dr}/\text{Å}}{\mathrm{dT}} \tag{6}$$

This result suggests that one can calculate dr/dT from the $^{1}H^{N}$ chemical shift and its temperature coefficient. Similarly, by assuming that dJ/dT arises solely from the hydrogen bond distance expansion, one can back calculate dr/dT from dJ/dT as well by taking temperature derivative on both sides of Eq. 1,

$$\frac{\mathrm{dJ}}{\mathrm{dT}} = -3.2\mathrm{J} \cdot \frac{\mathrm{dr}/\text{Å}}{\mathrm{dT}} \tag{7}$$

Although Eqs. 6 and 7 are simple, both have problems when applied to a real system. Equation 6 is derived from the MD simulation data and the coefficient 0.86 may not be applicable in reality. For Eq. 7, the measurement of $^{3h}J_{NC'}$ is very time consuming and the accurate determination of dJ/dT is difficult. Therefore, for most protein systems, using Eq. 7 to calculate dr/dT is unrealistic as well. Fortunately for GB3 the experimental dJ/dT is known, parameters in Eq. 4 can be refitted by using experimental dδ/dT and δ, as well as dr/dT calculated from Eq. 7 and dδ/dr from Eq. 5 to derive Eq. 8 which is applicable to a real system. The parameter $a = 0.43$ (Eq. 4) is obtained from the refit, smaller than that from MD; $b = -2.7 \times 10^{-4}$ (ppm/K), close to zero, is similar to MD (Fig. 5b). By setting $b = 0$, it is straightforward to show:

$$\frac{\mathrm{dr}}{\mathrm{dT}} = -\frac{1.16}{(\delta - 4.06\,\mathrm{ppm})} \cdot \frac{\mathrm{d}\delta}{\mathrm{dT}}\,\text{Å} \tag{8}$$

Equation 8 provides an empirical way to estimate the hydrogen bond distance thermal expansion coefficient dr/dT from the $^{1}H^{N}$ chemical shift and its temperature coefficient. But cautions need to be taken when applying Eq. 8 to calculate dr/dT. In deriving Eq. 8, we implicitly assume that dδ/dT arises exclusively from the hydrogen bond, so that other effects such as secondary structure, ring currents and electrostatics are not considered. Based on Fig. 3a and the early study of ubiquitin (Cordier and Grzesiek 2002), it is likely true. But for a specific residue, if the electrostatics changes due to the temperature increase, one has to consider such an effect in addition to the hydrogen bond. Another assumption is that dJ/dT and dδ/dT are mainly from the h-bond distance expansion dr/dT and a linear relationship exists between the two and dr/dT. The MD simulation data of GB3 support this assumption. But the direct experimental evidence is lacking.

The site specific values of dr/dT for protein GB3 were predicted using Eq. 8 and experimental dδ/dT. The average dr/dT is $7.9 \pm 5.1 \times 10^{-4}$ Å/K, comparable to that obtained for the protein ubiquitin, 5×10^{-4} Å/K derived from $^{3h}J_{NC'}$ values (Cordier and Grzesiek 2002). A rather large dr/dT variation is observed from site to site, ranging from -1.5×10^{-4} (A29) to 20.7×10^{-4} Å/K (A20). 30 out of 33 total h-bonded amides have positive values indicating the temperature increase weakens their hydrogen bonds, while the remaining three have negative values implying the corresponding hydrogen bonds are strengthened. These three amides are K28, A29 from helix α1 and V42 from strand β3. The strengthening of hydrogen bonds, observed before for ubiquitin (Cordier and Grzesiek 2002), reflects the complexity of intramolecular hydrogen bond network's response to temperature changes. Another possible cause for the three amides' negative dr/dT, or positive dδ/dT is the random coil population increase as the temperature increases (Andersen et al. 1997). The random coil $^{1}H^{N}$ chemical shifts are 8.33, 8.35 and 8.13 ppm for K, A and V (Kjaergaard et al. 2011). The GB3 chemical shifts for K28, A29 and V42 are 7.20, 7.24 and 8.26 ppm at 298 K. The small shift of the equilibrium toward the random coil conformation will increase the chemical shift of K28 and A29 and yield positive dδ/dT and negative dr/dT (same as the experiment), but decease the chemical shift of V42 (opposite to the experimental finding).

In an attempt to rationalize the dr/dT variations, dr/dT values were mapped on the GB3 3D structure (pdb: 2OED, Fig. 6). For the hydrogen bond network between β1 and β2, a pattern was identified. The dr/dT values are 14.8, 3.5, 7.4, 13.9×10^{-4} Å/K for Y3, L5, I7, G9 from β1 which are h-bonded to β2 as donors. The dr/dT for G14, T16, T18, A20 (from β2 hbonded to β1) are 9.5, 3.7, 6.8, 20.7×10^{-4} Å/K. Amides in middle part of the sheet have smaller dr/dT values, and are thus less extendable and more stable than amides at the edges. On the other hand, the hydrogen bond network formed by β3 and β4 shows a different dr/dT pattern. The three residues from β3 with amides h-bonded to β4 are E42, T44 and D46 with dr/dT −1.4, 15.3, 0.89×10^{-4} Å/K respectively, suggesting the edges are more restrained. The corresponding hydrogen bond partners from β4 are T51, T53 and T55, show a similar trend but less variation with dr/dT 5.2, 10.8, 10.3×10^{-4} Å/K. Another hydrogen bond network is formed between β1 and β4, including residues F52, V54 and E56 from β4 with dr/dT 8.0, 4.8, 15.3×10^{-4} Å/K as well as K4 and N8 from β1 with dr/dT 8.9, 5.3×10^{-4} Å/K. It appears that for this network, the middle part is more restricted. Unlike β strands, α1 helix shows no clear hydrogen bond expansion pattern (Fig. 6).

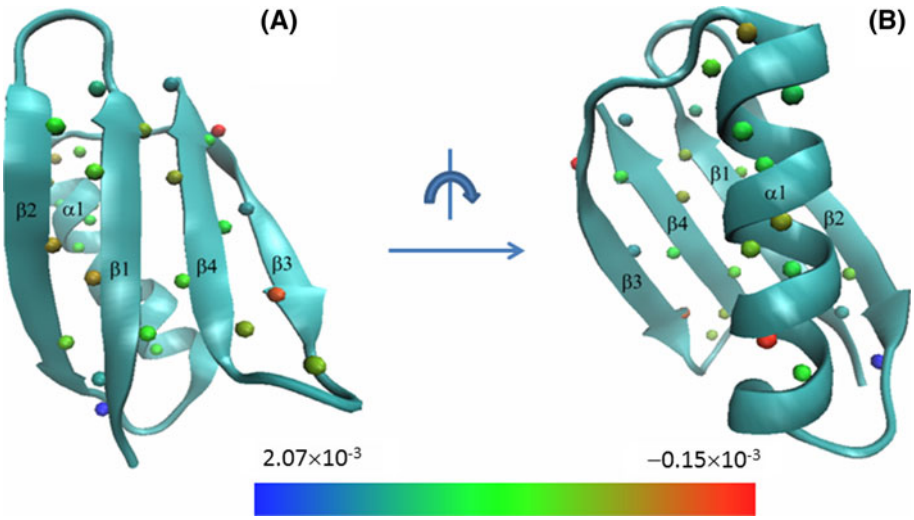

Fig. 6 Site-specific hydrogen bond distance temperature coefficient d*r*/d*T* mapped on the GB3 NMR structure (pdb code: 2OED). The backbone is shown with a ribbon diagram, amide $^{1}H^{N}$s are shown in a space-filling representation with the color depicting the value of d*r*/d*T*. **b** Back view of panel **a**. The figure was made using VMD (Humphrey et al. 1996)

Conclusion

The temperature dependence of the $^{1}H^{N}$ chemical shift was observed long ago (Ohnishi and Urry 1969), yet its mechanism is still not well understood. It has been suggested that the $^{1}H^{N}$ chemical shift temperature coefficient is related to the amide hydrogen bond strength (Cierpicki and Otlewski 2001; Cierpicki et al. 2002), the hydrogen bond expansion, or the equilibrium shift between the folded and unfolded conformations. In this study, we show that for a protein the $^{1}H^{N}$ chemical shift temperature coefficient reflects the effect of thermal expansion on the strength of hydrogen bond based on the observation that the $^{1}H^{N}$ temperature coefficient is nicely correlated to that of $^{3h}J_{NC'}$ for GB3 and ubiquitin. However, for individual residues the temperature dependent equilibrium shift between the ordered and disordered conformation may still contribute. Our computational results suggest that the hydrogen bond distance expansion is the main factor contributing to the $^{1}H^{N}$ chemical shift temperature dependence. An empirical equation was proposed to calculate the hydrogen bond distance temperature coefficient d*r*/d*T*. The predicted average d*r*/d*T* for GB3 is very small 7.9×10^{-4} Å/K, and is therefore undetectable by traditional structure determining techniques, e.g. X-ray electron diffraction or NMR NOE. These results reveal the exquisite sensitivity of $^{1}H^{N}$ chemical shift to hydrogen bond strength. d*r*/d*T* reflects the vibrational anharmonicity of the hydrogen bond, and disentangling this from the harmonic vibration, in principle, could provide more information about the enthalpic as well as entropic nature of the hydrogen bond.

Acknowledgments The authors would like to thank Dr. Dennis Torchia for the critical reading of the manuscript and Shanghai supercomputer center for the computer resources. This work was supported in part by 100 Talent Project of Chinese Academy of Sciences, National Nature Science Foundation of China (Grant no. 21173247) and the Foundation for Outstanding Young Scientist in Shandong Province (Grant no. JQ201104).

References

Andersen NH et al (1997) Extracting information from the temperature gradients of polypeptide NH chemical shifts.1. The importance of conformational averaging. J Am Chem Soc 119: 8547–8561

Barfield M (2002) Structural dependencies of interresidue scalar coupling (h3)J(NC), and donor H-1 chemical shifts in the hydrogen bonding regions of proteins. J Am Chem Soc 124: 4158–4168

Baxter NJ, Williamson MP (1997) Temperature dependence of H-1 chemical shifts in proteins. J Biomol NMR 9:359–369

Berendsen HJC (1991) Transport-properties computed by linear response through weak-coupling to a bath. Nato Adv Sci I E App 205:139–155

Cavalli A et al (2007) Protein structure determination from NMR chemical shifts. Proc Natl Acad Sci USA 104:9615–9620

Cierpicki T, Otlewski J (2001) Amide proton temperature coefficients as hydrogen bond indicators in proteins. J Biomol NMR 21: 249–261

Cierpicki T et al (2002) Hydrogen bonds in human ubiquitin reflected in temperature coefficients of amide protons. J Magn Reson 157:178–180

Cordier F, Grzesiek S (1999) Direct observation of hydrogen bonds in proteins by interresidue (3 h)J(NC′) scalar couplings. J Am Chem Soc 121:1601–1602

Cordier F, Grzesiek S (2002) Temperature-dependence properties as studied by of protein hydrogen bond high-resolution NMR. J Mol Biol 317:739–752

Cornilescu G, Hu JS, Bax A (1999a) Identification of the hydrogen bonding network in a protein by scalar couplings. J Am Chem Soc 121:2949–2950

Cornilescu G et al (1999b) Correlation between (3 h)J(NC′) and hydrogen bond length in proteins. J Am Chem Soc 121:6275–6279

Darden T, York D, Pedersen L (1993) Particle Mesh Ewald—an N.Log(N) method for Ewald Sums in large systems. J Chem Phys 98:10089–10092

Essmann U et al (1995) A smooth particle mesh ewald method. J Chem Phys 103:8577–8593
Grzesiek S et al (2004) Insights into biomolecular hydrogen bonds from hydrogen bond scalar couplings. Prog Nucl Magn Reson Spectrosc 45:275–300
Hansmann UHE (1997) Parallel tempering algorithm for conformational studies of biological molecules. Chem Phys Lett 281:140–150
Hess B et al (1997) LINCS: a linear constraint solver for molecular simulations. J Comput Chem 18:1463–1472
Hess B et al (2008) GROMACS 4: algorithms for highly efficient, load-balanced, and scalable molecular simulation. J Chem Theory Comput 4:435–447
Hornak V et al (2006) Comparison of multiple amber force fields and development of improved protein backbone parameters. Proteins Struct Funct Bioinform 65:712–725
Humphrey W, Dalke A, Schulten K (1996) VMD: visual molecular dynamics. J Mol Graph Model 14:33–38
Kjaergaard M, Brander S, Poulsen FM (2011) Random coil chemical shift for intrinsically disordered proteins: effects of temperature and pH. J Biomol NMR 49:139–149
Kohlhoff KJ et al (2009) Fast and accurate predictions of protein nmr chemical shifts from interatomic distances. J Am Chem Soc 131:13894–13895
Miyamoto S, Kollman PA (1992) Settle: an analytical version of the shake and rattle algorithm for rigid water models. J Comput Chem 13:952–962
Neal S et al (2003) Rapid and accurate calculation of protein H-1, C-13 and N-15 chemical shifts. J Biomol NMR 26:215–240
Ohnishi M, Urry DW (1969) Temperature dependence of amide proton chemical shift: secondary structures of gramicidin s and valinomycin. Biochem Bioph Res Co 36:194–202
Parker LL, Houk AR, Jensen JH (2006) Cooperative hydrogen bonding effects are key determinants of backbone amide proton chemical shifts in proteins. J Am Chem Soc 128:9863–9872
Patriksson A, van der Spoel D (2008) A temperature predictor for parallel tempering simulations. Phys Chem Chem Phys 10:2073–2077
Sass H-J, Schmid FF-F, Grzesiek S (2007) Correlation of protein structure and dynamics to scalar couplings across hydrogen bonds. J Am Chem Soc 129:5898–5903
Shen Y, Bax A (2007) Protein backbone chemical shifts predicted from searching a database for torsion angle and sequence homology. J Biomol NMR 38:289–302
Shen Y, Bax A (2010) SPARTA plus: a modest improvement in empirical NMR chemical shift prediction by means of an artificial neural network. J Biomol NMR 48:13–22
Shen Y et al (2008) Consistent blind protein structure generation from NMR chemical shift data. Proc Natl Acad Sci USA 105:4685–4690
Shen Y et al (2009) TALOS plus: a hybrid method for predicting protein backbone torsion angles from NMR chemical shifts. J Biomol NMR 44:213–223
Sitkoff D, Case DA (1997) Density functional calculations of proton chemical shifts in model peptides. J Am Chem Soc 119:12262–12273
Sugita Y, Okamoto Y (1999) Replica-exchange molecular dynamics method for protein folding. Chem Phys Lett 314:141–151
Tomlinson JH, Williamson MP (2012) Amide temperature coefficients in the protein G B1 domain. J Biomol NMR 52:57–64
Van der Spoel D et al (2005) GROMACS: fast, flexible, and free. J Comput Chem 26:1701–1718
Vila JA et al (2008) Quantum chemical C-13(alpha) chemical shift calculations for protein NMR structure determination, refinement, and validation. Proc Natl Acad Sci USA 105:14389–14394
Xu XP, Case DA (2001) Automated prediction of (15)N, (13)C(alpha), (13)C(beta) and (13)C′ chemical shifts in proteins using a density functional database. J Biomol NMR 21:321–333
Yao L, Ying J, Bax A (2009) Improved accuracy of N-15-H-1 scalar and residual dipolar couplings from gradient-enhanced IPAP-HSQC experiments on protonated proteins. J Biomol NMR 43: 161–170